

Document downloaded from:

<http://hdl.handle.net/10251/120241>

This paper must be cited as:

Llopis-Castelló, D.; Camacho-Torregrosa, FJ.; García García, A. (2018). Development of a global inertial consistency model to assess road safety on Spanish two-lane rural roads. *Accident Analysis & Prevention*. 119(October 2018):138-148.  
<https://doi.org/10.1016/j.aap.2018.07.018>



The final publication is available at

<https://doi.org/10.1016/j.aap.2018.07.018>

Copyright Elsevier

Additional Information

1 **DEVELOPMENT OF A GLOBAL INERTIAL CONSISTENCY MODEL TO ASSESS ROAD**  
2 **SAFETY ON SPANISH TWO-LANE RURAL ROADS**

3  
4 Corresponding Author:

5 **David Llopis-Castelló**

6 PhD Researcher

7 Highway Engineering Research Group (HERG)

8 Universitat Politècnica de València

9 Camino de Vera, s/n 46022, Valencia, Spain

10 Tel: (34) 96 3877374

11 E-mail: dallocas@doctor.upv.es

12  
13 Other Authors:

14 **Francisco Javier Camacho-Torregrosa**

15 Assistant Professor

16 HERG

17 Universitat Politècnica de València

18 E-mail: fracator@tra.upv.es

19  
20 **Alfredo García**

21 Professor

22 HERG

23 Universitat Politècnica de València

24 E-mail: agarciag@tra.upv.es

25  
26  
27 Submission Date: 11<sup>th</sup> December 2017

28 **ABSTRACT**

29 The most important factors for road crash occurrence are infrastructure, vehicle, and human factors. In fact,  
30 infrastructure and its interaction with human factor have been thoroughly studied in recent years through  
31 geometric design consistency, which can be defined as how drivers' expectations and road behavior relate.

32 Global consistency models were calibrated in the last decade to assess road safety on an entire  
33 homogeneous road segment. However, none of them include the underlying consistency phenomenon in  
34 their formulation.

35 Recently, a new model was developed based on the difference between the inertial operating speed  
36 profile, which represents drivers' expectancies, and the operating speed profile, which represents road  
37 behavior. While the operating speed represents the estimated operating speed for every location along the  
38 road, the inertial operating speed aggregates for every station the operating speed effect along some distance  
39 already covered by drivers. The authors hypothesized that this 'aggregation effect' was connected to drivers'  
40 expectancies, which proved to be true based on the best model fitted. However, the exact distance (or time)  
41 that should be considered to estimate the inertial operating speed still remains unknown. This paper aims  
42 to complete this model, analyzing how the inertial operating speed varies depending on different distances  
43 and periods of time. This impact is measured considering the reliability of the corresponding consistency  
44 model. The paper also covers how the inertial operating speed should be determined along the final distance  
45 or time. For this, a total of 184 homogeneous road segments along 650 kilometers in Spain were used.

46  
47 *Keywords: geometric design consistency, road safety, operating speed, inertial operating speed, driver's*  
48 *behavior*

## 49 1. INTRODUCTION

50 Road safety is one of the major concerns in our society. In fact, approximately 1.2 million people die and  
51 50 million are injured in road crashes every year. This makes road crashes the main cause of death for  
52 people aged 15-29 (WHO, 2015).

53 In Spain, 1,291 fatalities occurred on rural roads in 2016, of which more than 70% occurred on  
54 two-lane rural roads. Although the number of crashes has been in decline on rural roads since the beginning  
55 of the century, the fatalities have increased in recent years on two-lane rural roads. In addition, this type of  
56 road represents approximately 90% of the road network in this country, so two-lane rural roads play a  
57 pivotal role in road safety (DGT, 2017).

58 The most important factors for road crash occurrence are infrastructure, vehicle, and human factors.  
59 Particularly, the infrastructure factor is responsible for over 30% of road crashes (Treat et al., 1979). In fact,  
60 crashes tend to concentrate at certain road elements. For this, infrastructure and its interaction with human  
61 factor have been thoroughly studied in recent years through geometric design consistency, which can be  
62 defined as how drivers' expectations and road behavior relate.

63 Road behavior can be defined as the general performance of its alignment (e.g. sharpness, design  
64 speed, etc.). Drivers tend to perform according to the road geometry, but the expectancies based on the road  
65 segment immediately covered also play an important role. Thus, a consistent road provides a harmonious  
66 driving free of surprises, whereas an inconsistent road design might produce numerous unexpected events  
67 to drivers, leading to anomalous behavior and increasing the likelihood of crash occurrence.

68 Among the different methods to assess geometric design consistency, the most commonly used is  
69 based on the analysis of the operating speed profile (Gibreel et al., 1999). Operating speed is frequently  
70 defined as the 85<sup>th</sup> percentile of the speed distribution for passenger cars under free-flow conditions with  
71 no external restrictions ( $V_{85}$ ). One important advantage of its use is the possibility to estimate it using  
72 operating speed models.

73 There are two types of consistency models: local and global. Local models focus on localized issues,  
74 such as sudden speed reductions or large differences between the design and operating speeds. Those

75 models are ideal to identify where road crashes are more likely to occur. On the other hand, global  
76 consistency models examine the overall speed variation throughout an entire road segment. Although they  
77 do not indicate where crashes are prone to take place, they can be introduced into a Safety Performance  
78 Function (SPF) to predict the number of crashes on an entire road segment.

79 To this regard, several researchers have tried to relate the number of crashes to different variables  
80 related to risk exposure (traffic volume and road length), geometry, consistency, and road environment by  
81 means of SPFs. Among those studies which incorporate the consistency as an explanatory variable, all of  
82 them concluded that the level of consistency has a major influence on road crash occurrence (Anderson et  
83 al., 1999; Ng and Sayed, 2004; Awatta et al., 2006; Montella et al., 2008; Cafiso et al., 2010; de Oña et al.,  
84 2013; Quddus, 2013; Wu et al., 2013; Garach et al., 2014; Camacho-Torregrosa, 2015; Montella and  
85 Imbriani, 2015; Garach et al., 2016).

86 The first global consistency model was developed by Polus and Mattar-Habib (2004), which was  
87 based on two parameters: relative area ( $Ra$ ) and operating speed dispersion ( $\sigma$ ). The first parameter was  
88 defined as the area bounded by the operating speed profile and the average operating speed, divided by the  
89 length of the road segment. The same parameters were used by Garach et al. (2014) to calibrate a new  
90 consistency model on Spanish two-lane rural roads (Table 1).

91 Later, Camacho-Torregrosa (2015) developed another global consistency model considering two  
92 operational parameters: the average operating speed ( $\overline{V_{85}}$ ) and the average deceleration rate ( $\overline{d_{85}}$ ). The first  
93 parameter is the average value of the operating speed along the entire road segment, measured in m/s. The  
94 second one is the average value of the decelerations of the same operating speed profile, in m/s<sup>2</sup>.  
95 Additionally, this research analyzed the influence of the selection of homogeneous road segments on the  
96 estimation of road crashes (Table 1).

97 Regarding this, the selection of the road segment is critical for the application of global consistency  
98 models. Selected road segments must be homogeneous, because the results depend on its selection (Resende  
99 and Benekohal, 1997; Cafiso et al., 2010; García et al., 2013a; Camacho Torregrosa, 2015).

101 **TABLE 1 Previous global consistency models**

Global consistency model	Consistency parameter (C)	Consistency level		
		Good	Fair	Poor
Polus and Mattar-Habib (2004)	$2.808 \cdot e^{-0.278 \cdot Ra \cdot \frac{\sigma}{3.6}}$	$C > 2$	$1 < C \leq 2$	$C \leq 1$
Garach et al. (2014)	$\frac{195.073}{\left(\frac{\sigma}{3.6} - 5.7933\right) \cdot (4.1712 - R_a) - 26.6047} + 6.7826$	$C > 2$	$1 < C \leq 2$	$C \leq 1$
Camacho-Torregrosa (2015)	$\sqrt[3]{\frac{V_{85}}{d_{85}}} \quad (s^{1/3})$	$C \geq 3.25$	$2.55 \leq C < 3.25$	$C < 2.55$

102

103 However, none of these consistency models include the underlying consistency phenomenon in  
104 their formulation, i.e., they do not contain a variable which represents and estimates drivers' expectancies.

105 To this regard, García et al. (2013b) defined a new speed concept: the inertial operating speed ( $V_i$ ).  
106 This speed is used to represent drivers' expectancies and was defined as the average operating speed along  
107 the preceding 1,000 m road segment. Conversely, road behavior was associated with the operating speed  
108 ( $V_{85}$ ). A new local consistency parameter, the Inertial Consistency Index (ICI), was defined as the difference  
109 between  $V_i$  and  $V_{85}$ . Therefore, the larger this index, the greater the difference between drivers' expectancies  
110 and road behavior, being crashes more likely to appear.

111 However, this definition of the inertial operating speed does not match the drivers' expectancies  
112 acquirement process, which is closely related to Short-Term Memory (STM). To this regard, STM is  
113 gradually in decline over time, being the information lost in approximately 18 seconds (Revlin, 2012).

114 Drivers do not recall with the same intensity all locations of the previous road section. Therefore,  
115 the first and final parts of the section should not be equally considered to determine the inertial operating  
116 speed. In addition, given two homogeneous road segments with different average operating speeds, the  
117 periods of time needed to cover the same distance differ.

118 Recent studies have been used to identify how the inertial operating speed should be calculated on  
119 Italian two-lane rural roads (Llopis-Castelló et al., 2017 and 2018). As a conclusion, an inertial operating  
120 speed estimated as the weighted average operating speed based on time was able to better represent drivers'  
121 expectancies than a  $V_i$  based on distance and calculated as a simple average of the operating speed. In  
122 addition, a global consistency model was developed based on the difference between the inertial operating  
123 speed profile and the operating speed profile. As a result, this consistency model allowed a more accurate

124 estimation of the number of crashes than the previous global models mentioned above.

125         Due to the successful performance of the inertial consistency models calibrated in Italy, this study  
126 presents an attempt to enhance the accuracy of the estimation of the inertial operating speed by examining  
127 a greater number of road sections and considering more weighting distributions. As a result, a new global  
128 consistency model is presented.

## 129 **2. OBJECTIVES AND HYPOTHESES**

130 The main objective of this research is to develop a new global consistency model comparing the difference  
131 between the inertial operating speed and the operating speed with the number of crashes on Spanish two-  
132 lane rural roads.

133         To this regard, the inertial operating speed was studied considering new weighting distributions to  
134 get as close as possible to Short-Term Memory behavior. This will allow identifying how the inertial  
135 operating speed should be calculated to estimate drivers' expectancies in a more accurate way.

136         The underlying hypothesis is that an inertial operating speed profile based on time will allow a  
137 more accurate estimation of the number of crashes than those based on distance. Likewise, the greater the  
138 difference between inertial operating speed profile and operating speed profile, the worse the consistency.

## 139 **3. METHODOLOGY AND DATA DESCRIPTION**

### 140 **3.1. Methodology**

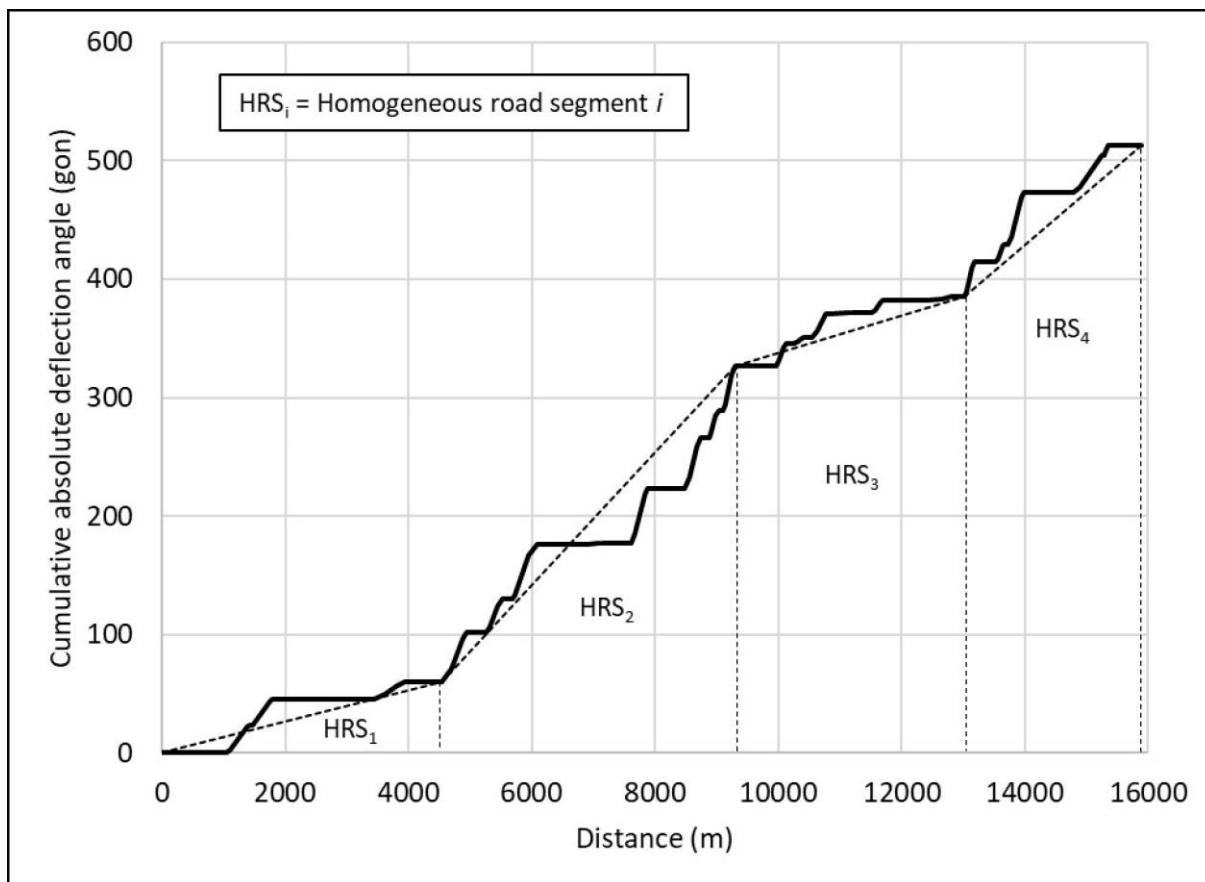
141 The methodology of this study was similar to those used in Llopis-Castelló et al. (2018a and 2018b). Two-  
142 lane rural road sections were selected. Next, the geometry for each road section was recreated by means of  
143 the methodology proposed by Camacho-Torregrosa et al. (2015), which uses an algorithm based on the  
144 heading direction. The operating speed profiles were estimated considering the models developed by Pérez-  
145 Zuriaga (2012), which were calibrated for Spanish two-lane rural roads with the same characteristics than  
146 those road sections considered in this research. From this, different inertial operating speed profiles were  
147 calculated for each road segment considering different distances, periods of time, and weighting  
148 distributions. Crash and traffic data were also obtained. Finally, the relationship between crashes and  
149 consistency was studied calibrating several Safety Performance Functions. As a result, the inertial operating

150 speed profile that better represents drivers' expectancies was identified, and consistency thresholds were  
 151 defined.

### 152 3.2. Road segments

153 A total of 98 two-lane rural road sections located in the Valencian Region (Spain) were selected for the  
 154 study. This required the geometric recreation of more than 650 km of highway resulting in 184  
 155 homogeneous road segments, which were identified by means of the following procedure.

156 First, road segments were divided into sections with similar traffic volume and cross-section. Major  
 157 intersections also influence drivers' expectancies, so they were also considered for segmentation. Finally,  
 158 each road section was divided according to its geometric behavior using the German methodology, which  
 159 is based on the analysis of the Curvature Change Rate (*CCR*). This parameter is defined as the rate between  
 160 the sum of the absolute deflection angles and the length of the road segment. Figure 1 shows how this last  
 161 step is carried out: a profile of the cumulative absolute deflection angle versus the road station must be  
 162 plotted. In this way, homogeneous road segments can be distinguished according to similar *CCR* behavior.



163



164 **FIGURE 1 Identification of homogeneous road segments.**

165 Table 2 shows the main geometric characteristics of the studied homogeneous road segments. In  
 166 addition, most of them present similar cross-section features with lane widths between 3.00 and 3.50 m,  
 167 and shoulder widths between 0.5 and 1.50 m. Their longitudinal grade did not exceed 5%.

168 **TABLE 2 Statistical summary of the homogeneous road segments**

	Minimum	Maximum	Average	Standard deviation
Length (m)	1,146	10,851	3,535	1,593
CCR (gon/km)	0	1,078	209	101.91
AADT (vpd)	465	10,817	2,641	2,065
Crashes	0	48	7.57	7.53

169 **3.3. Traffic and crash data**

170 Traffic volume and crash data were provided by the Department of Housing, Public Works, and Spatial  
 171 Planning of the Valencian Regional Government and the General Directorate of Traffic (Dirección General  
 172 de Tráfico, DGT) of the Spanish Government, respectively. Thus, the Annual Average Daily Traffic (*AADT*)  
 173 volumes and the number of fatal-and-injury crashes were identified for each homogeneous road segment.

174 *AADT* was defined as the average traffic volume from 2002 to 2011. In this way, the homogeneous  
 175 road segments presented an *AADT* ranging from 465 to 10,817 vpd (Table 2). Additionally, the variability  
 176 of the traffic volume over time was analyzed through the coefficient of variation (*CV*) for each  
 177 homogeneous road segment. As a result, the mean *CV* and its standard deviation were 21% and 10%,  
 178 respectively. Therefore, the traffic variation along the studied years can be considered low.

179 Only fatal-and-injury crashes were considered in the same period of time. The cause of every crash  
 180 was reviewed to only include those related to geometry (e.g., crashes caused by vehicles entering the road  
 181 from minor roads or driveways were removed from the analysis, since their cause is not the road geometry  
 182 per se). As a result, a total of 1,392 reported crashes were considered (Table 2).

183 **3.4. Speed profiles**

184 3.4.1. Operating speed profiles

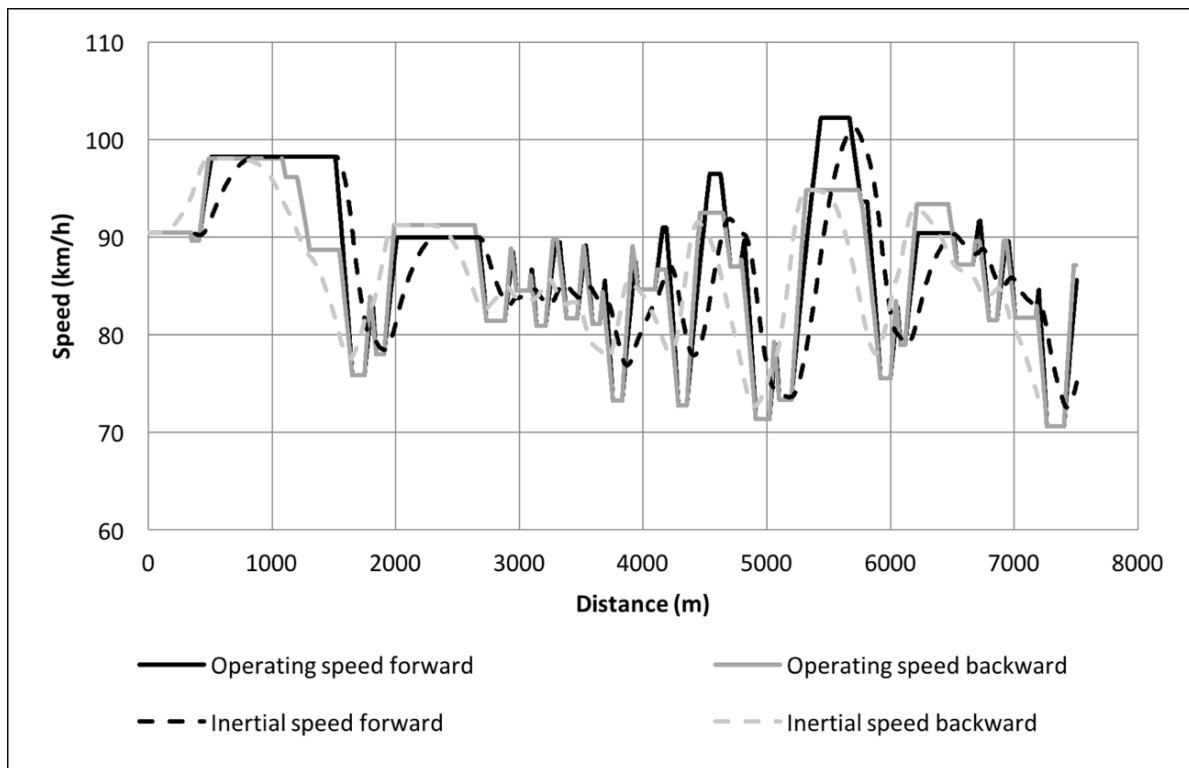
185 The operating speed profile for each road segment was estimated using the operating speed profile model  
 186 developed by Pérez-Zuriaga (2012), which was calibrated based on speed data collected on Spanish two-  
 187 lane rural roads with the same characteristics of the road sections considered in this study (Table 3). As a

188 result, the operating speed was obtained meter by meter (Figure 2).

189 **TABLE 3 Speed models developed by Pérez-Zuriaga (2012)**

Type of road element	Equation
Horizontal curve	$V_{85,C} = 106.863 - 60.1185/e^{0.00422596 \cdot R}$
Tangent	$L \geq 700 \text{ m}$ $V_{85,T} = \sqrt{-1,464.72 + 351.288 \cdot \sqrt{L}}$
	$L < 700 \text{ m} \ \& \ R_l \leq 600 \text{ m}$ $V_{85,T} = 0.362739 \cdot V_{85,C1} + 59.6982/e^{-0.0000472302 \cdot GM}$
	$L < 700 \text{ m} \ \& \ R_l > 600 \text{ m}$ $V_{85,T} = \sqrt{7,399.27 + 3.03956 \cdot L}$
Acceleration rate	$a_{85} = 1/(-1.49325 + 0.548458 \cdot \ln(R))$
Deceleration rate	$d_{85} = \sqrt{-0.0652071 + 201.174/R}$
<p>where <math>V_{85,C}</math> is the operating speed on horizontal curves (km/h); <math>V_{85,T}</math> is the operating speed on tangents (km/h); <math>a_{85}</math> is the acceleration rate (<math>\text{m/s}^2</math>); <math>d_{85}</math> is the deceleration rate (<math>\text{m/s}^2</math>); <math>V_{85,C1}</math> is the operating speed on the previous horizontal curve (km/h); <math>R</math> is the radius of the horizontal curve (m); <math>R_l</math> is the radius of the previous horizontal curve (m); <math>R_2</math> is the radius of the successive horizontal curve (m); <math>L</math> is the length of the tangent (m); and <math>GM</math> is the following geometric index (<math>\text{m}^2</math>):</p> $GM = \frac{L \cdot (R_1 \cdot R_2)^{0.5}}{100}$	

190



191  
192

**FIGURE 2 Speed profiles**

## 193 3.4.2. Inertial speed profiles

194 The inertial operating speed profile was calculated for every road segment on the basis of its operating  
 195 speed profile. To do this, the inertial operating speed was calculated for every station as the weighted  
 196 average operating speed of the preceding road section by means of the following equation:

$$197 \quad V_{i,k} = \frac{\sum w_j \cdot V_{85,j}}{\sum w_j} \quad (1)$$

198 where  $V_{i,k}$  is the inertial operating speed (km/h) at station  $k$ ;  $V_{85,j}$  is the operating speed at station  $j$ ; and  $w_j$   
 199 is the weighting factor at point  $j$ . Depending on the range covered by  $j$ , the result of the operating speed will  
 200 vary.

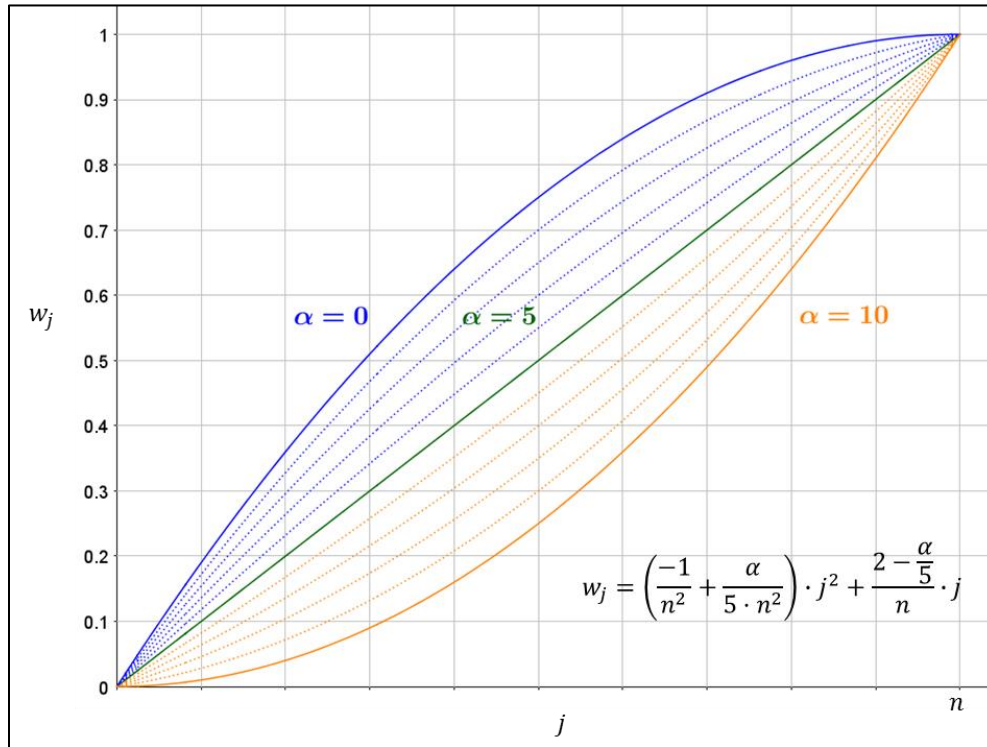
201 Inertial operating speeds were determined with the following distance and time parameters:

- 202 • Distances ( $L$ ) between 300 m and 800 m with a step of 100 m
- 203 • Periods of time ( $t$ ) between 10 s and 40 s, with a step of 5 s

204 In addition, 11 weighting distributions were considered. The weighting distributions were based on  
 205 a parabolic functional form ( $ax^2+bx+c$ ). These distributions could take values from 0 to 1, increasing as the  
 206 station  $j$  gets closer to the critical section  $k$ , with these constraints:

- 207 •  $w_j = 0$  for the first station  $j$  considered for the calculation. It is the threshold between the zone that  
 208 has not been included in the calculation (because it has no influence on driver's behavior), and the  
 209 zone under consideration.
- 210 •  $w_j = 1$  for  $j = k$ . It means that the station where the driver actually is located at a certain moment  
 211 has to be the most important for the expectancy formation.

212 As a result, the parabolic function can only take certain  $a$ ,  $b$ , and  $c$  parameters. Moreover, it can be  
 213 rewritten as a function of a single parameter  $\alpha$ , which varies between 0 and 10 (Figure 3). In this equation,  
 214  $n$  is the number of intervals considered in the calculation. The number of the intervals ( $n$ ) depended on  
 215 whether the calculation was carried out considering a distance ( $L$ ), in meters; or a period of time ( $t$ ), in  
 216 seconds. In the first case,  $n$  was equal to  $L$  (i.e., the calculation was performed meter by meter), whereas in  
 217 the second case,  $n$  was equal to  $10 \cdot t$ , so the inertial operating speed was calculated considering intervals of  
 218 0.1 s.



219  
220 **FIGURE 3 Weighting distributions.**

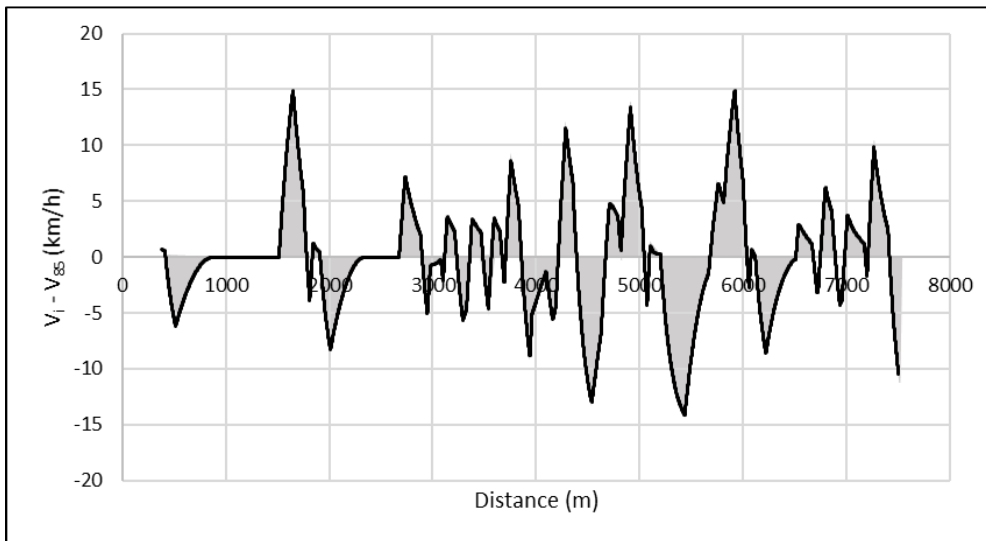
221 As a result, 143 ((6 distances + 7 periods of time) x (11 weighting distributions)) inertial operating  
 222 speed profiles were obtained for each homogeneous road segment. As an example, Figure 2 shows the  
 223 operating speed profile and its corresponding inertial operating speed profile considering 15 s and a linear  
 224 weighting distribution for one of the road segments under study.

### 225 3.5. Consistency parameters

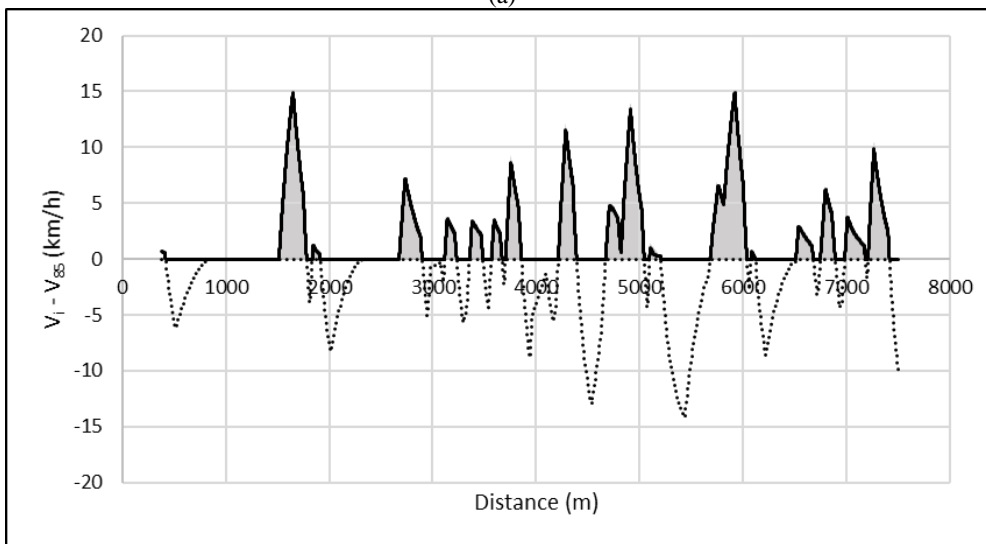
226 The consistency parameters depend on several variables defined from the difference between  $V_i$  and  $V_{85}$   
 227 (Llopis-Castelló et al., 2017 and 2018). As an example, Figure 4 shows the speed differences between both  
 228 speed profiles only considering forward direction. According to this definition, a positive difference means  
 229 that drivers' expectancies might not be achieved, because drivers' speed is lower than the speed they were  
 230 maintaining in the last section. Therefore, the likelihood of crashes increases with the magnitude of these  
 231 differences.

232 The consistency parameters were based on the combination of the following, simpler parameters  
 233 for every road segment (Figure 4):

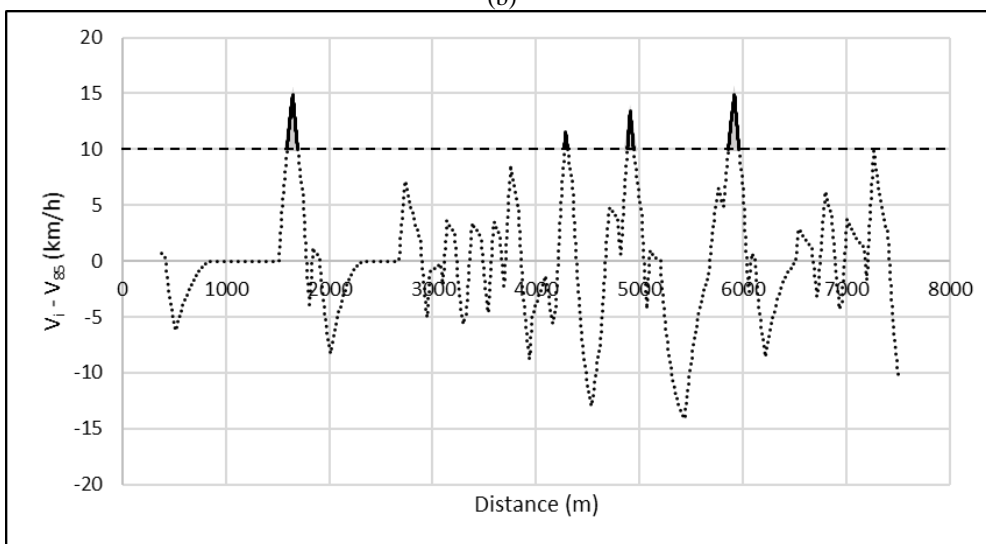
- 234 •  $A$  (m·km/h): area bounded by the difference between  $V_i$  and  $V_{85}$ , and the x axis (shaded area in  
235 Figure 4a).
- 236 •  $L$  (m): length of the road segment.
- 237 •  $\sigma$  (km/h): standard deviation of the difference between  $V_i$  and  $V_{85}$  (standard deviation of the  
238 profile in Figure 4a).
- 239 •  $A(+)$  (m·km/h): area bounded by the difference between  $V_i$  and  $V_{85}$  considering only the positive  
240 differences (shaded area in Figure 4b).
- 241 •  $L(+)$  (m): length of the road segment considering only the positive differences between  $V_i$  and  $V_{85}$   
242 (length of the road segment highlighted in Figure 4b).
- 243 •  $\sigma(+)$  (km/h): standard deviation of the difference between  $V_i$  and  $V_{85}$  considering only the positive  
244 differences (standard deviation of the profile in Figure 4b).
- 245 •  $A(> x \text{ km/h})$  (m·km/h): area bounded when the difference between  $V_i$  and  $V_{85}$  is higher than  $x$   
246 km/h (shaded area in Figure 4c).
- 247



(a)



(b)



(c)

248  
249

**FIGURE 4 Consistency variables: (a) A, L and  $\sigma$ ; (b) A(+), L(+) and  $\sigma$ (+); and (c) A(> x km/h).**

250 Table 4 summarizes the consistency parameters (Llopis-Castelló et al., 2017 and 2018). All of them  
 251 are expressed in terms of speed (km/h), making their interpretation easier compared to other consistency  
 252 models. In all cases, a higher value of the parameter indicates a lower consistency level.

253 **TABLE 4 Consistency parameters**

Parameter	Equation
1	$\sqrt{\frac{A(+)\cdot\sigma}{L}} [km/h]$
2	$\sqrt{\frac{A\cdot\sigma}{L}} [km/h]$
3	$\frac{A(+)}{L(+)} [km/h]$
4	$\frac{A(> 10 km/h)}{L} [km/h]$
5	$\frac{A(> 15 km/h)}{L} [km/h]$
6	$\frac{A(> 20 km/h)}{L} [km/h]$
7	$\sqrt{\frac{A(+)\cdot\sigma(+)}{L(+)}} [km/h]$
8	$\sqrt{\frac{A(+)\cdot\sigma}{L(+)}} [km/h]$

254

#### 255 4. ANALYSIS

256 A total of 1,144 Safety Performance Functions (SPF) were calibrated to identify how the inertial operating  
 257 speed should be calculated. This was the result of the combination of the 143 inertial operating speed  
 258 profiles and 8 consistency parameters.

259 A SPF is an expression that relates risk exposure and consistency to the number of crashes.  
 260 Following common practice, generalized linear modelling techniques were used to fit these functions  
 261 (Equation 2), and a negative binomial distribution was assumed, since it is an appropriate solution with  
 262 overdispersed, count data (Lord et al., 2010).

$$263 Y_{i,10} = e^{\beta_0} \cdot L^{\beta_1} \cdot AADT^{\beta_2} \cdot e^{\beta_3 C} \quad (2)$$

264 where  $Y_{i,10}$ : fatal-and-injury crashes on the road segment in 10 years;  $\beta_i$ : regression coefficients;  $L$ : length

265 of the road segment (km); *AADT*: Average Annual Daily Traffic (vpd); and *C*: consistency parameter (km/h).

266 In this expression, *AADT* is not set as an offset variable (i.e., crash rate decreases with traffic  
267 volume, which is generally accepted and meets SPFs developed by other researchers). However, the length  
268 is neither set as an offset variable, which is quite more controversial. At a first glance, this expression form  
269 is not adequate, since the estimated amount of crashes depends on how the road network is divided into  
270 road segments. This controversial expression has also been used by other researchers (Mehta and Lou,  
271 2013; Srinivasan et al., 2016; Garach et al., 2016; Camacho-Torregrosa, 2015; Llopis-Castelló et al., 2018a  
272 and 2018b). The key is that SPFs not showing the length as an offset variable must also indicate how the  
273 road network should be divided into road homogeneous segments – thus, there is just a single possible  
274 outcome of road crashes. In fact, Camacho-Torregrosa (2015) demonstrated that more accurate SPFs could  
275 be calibrated considering the length as an elasticity term. Furthermore, he classified homogeneous road  
276 segments into two categories: constrained and free. Constrained road segments are those that begin – or end  
277 – in an urban zone or major intersection. Otherwise, the road segment is free. Therefore, at constrained road  
278 intersections drivers are aware of entering into a new road segment, with new characteristics. As a result,  
279 they subconsciously pay more attention to the road behavior (in order to create their new expectancies),  
280 leading to lower crash rates. After some distance, this expectancy-acquisition process vanishes, so crash  
281 rates increase. This leads to a SPF in which the exponent affecting the length is higher than 1. On the other  
282 hand, at the beginning of free road segments, drivers are not aware of the change of the road segment, so  
283 they compare the new road behavior to the ad hoc expectancies formed along the previous road segment.  
284 Therefore, more crashes are expected at the beginning of these kind of road segments. After travelling some  
285 distance, they readapt their expectancies to the new road behavior, so crash rates tend to decrease. Therefore,  
286 the exponent affecting the length was found to be lower than 1. In fact, for long road segments, the crash  
287 rate outcome was found to be nearly the same for free and constrained road segments.

288 The *AIC* (Akaike Information Criterion) index was obtained for all regressions as a measure of  
289 goodness of fit. The smaller the *AIC* value, the better the model. Additionally, the Root Mean Square Error  
290 (*RMSE*) and the Mean Absolute Error (*MAE*) were calculated for the most accurate models (Table 5).



291 However, it is well known that crashes are highly affected by the exposure. Thus, a single-exposure  
292 SPF was previously calibrated to determine how important the inclusion of the consistency term is for crash  
293 prediction:

$$294 \quad y_{i,10} = e^{-5.05097} \cdot L^{0.84111} \cdot AADT^{0.76993} \quad AIC = 998.97 \quad (3)$$

295 To this regard, most of the calibrated SPFs which jointly considered risk exposure and consistency  
296 produced a lower *AIC* value than the single-exposure SPF, so the level of consistency had a major influence  
297 on road crash occurrence.

298 The consistency parameters showing better results were parameters 7 and 8. These parameters were  
299 mainly obtained by means of the positive differences between the inertial operating speed profile and the  
300 operating speed profile. The only difference between both parameters was that parameter 7 was calculated  
301 considering  $\sigma(+)$ , whereas parameter 8 depended on  $\sigma$  (Table 4). This meant that the positive difference  
302 between both speed profiles was able to represent where drivers' expectancies were not achieved. Although  
303 parameter 8 showed lower *AIC* values than parameter 7, parameter 7 presented the lowest values of *RMSE*  
304 and *MAE* (Table 5).

305 Regarding the calculation of the inertial operating speed, different segment lengths resulted in  
306 reasonable results. To analyze this phenomenon more thoroughly, the homogeneous road segments were  
307 divided into free and constrained segments according to Camacho-Torregrosa (2015). In this way,  
308 constrained road segments showed better results using 500 m, whereas free segments performed better with  
309 400 m (Table 5).

310 However, the best results regarding time did not depend on the type of road segment. To this regard,  
311 the inertial operating speed profile was calculated considering 15 s.

312 Therefore, a time-based inertial operating speed profile led more consistent results than the  
313 calculation of this profile based on distance. This might be due to the mean operating speed, which was  
314 different for each type of road segment. Then, different distances are achieved for the same period of time.

315 Finally, the weighting distributions were studied. As a conclusion, the best consistency models used  
316 weighting distributions with values of the parameter  $\alpha$  between 5 and 10.

317 **TABLE 5 Best consistency models**

(a) All road segments										
Model*	Consistency parameter		$\beta_0$ -	$\beta_1$ $\ln L$	$\beta_2$ $\ln AADT$	$\beta_3$ $C$	Overdispersion $\theta$	AIC	RMSE	MAE
L <sub>500,5</sub>	7	Estimate Pr(> z )	-13.4366 < 2·10 <sup>-16</sup>	1.01182 < 2·10 <sup>-16</sup>	0.83972 < 2·10 <sup>-16</sup>	0.1322 4.58·10 <sup>-8</sup>	6.07	974.02	4.27	3.03
t <sub>15,10</sub>	7	Estimate Pr(> z )	-13.7030 < 2·10 <sup>-16</sup>	1.02146 < 2·10 <sup>-16</sup>	0.85711 < 2·10 <sup>-16</sup>	0.18027 1.99·10 <sup>-7</sup>	6.04	976.06	4.21	3.04
L <sub>500,5</sub>	8	Estimate Pr(> z )	-14.0447 < 2·10 <sup>-16</sup>	1.04579 < 2·10 <sup>-16</sup>	0.88047 < 2·10 <sup>-16</sup>	0.11514 2.3·10 <sup>-8</sup>	6.08	972.64	4.32	3.07
t <sub>15,10</sub>	8	Estimate Pr(> z )	-14.1939 < 2·10 <sup>-16</sup>	1.04805 < 2·10 <sup>-16</sup>	0.89429 < 2·10 <sup>-16</sup>	0.15059 6.85·10 <sup>-8</sup>	6.00	974.49	4.30	3.11
Single-Exposure	-	Estimate Pr(> z )	-10.8612 < 2·10 <sup>-16</sup>	0.8411 6.77·10 <sup>-14</sup>	0.76993 < 2·10 <sup>-16</sup>	- -	4.57	998.97	4.78	3.45
(b) Constrained road segments										
Model	Consistency parameter		$\beta_0$ -	$\beta_1$ $\ln L$	$\beta_2$ $\ln AADT$	$\beta_3$ $C$	Overdispersion $\theta$	AIC	RMSE	MAE
L <sub>500,5</sub>	7	Estimate Pr(> z )	-13.7677 < 2·10 <sup>-16</sup>	1.04793 < 2·10 <sup>-16</sup>	0.84720 < 2·10 <sup>-16</sup>	0.12926 4.71·10 <sup>-6</sup>	5.22	771.64	4.71	3.41
t <sub>15,10</sub>	7	Estimate Pr(> z )	-14.0603 < 2·10 <sup>-16</sup>	1.06023 < 2·10 <sup>-16</sup>	0.86447 < 2·10 <sup>-16</sup>	0.17752 1.37·10 <sup>-5</sup>	5.17	773.41	4.66	3.43
L <sub>500,5</sub>	8	Estimate Pr(> z )	-14.2337 < 2·10 <sup>-16</sup>	1.07095 < 2·10 <sup>-16</sup>	0.88229 < 2·10 <sup>-16</sup>	0.11156 2.72·10 <sup>-6</sup>	5.21	770.95	4.78	3.45
t <sub>15,10</sub>	8	Estimate Pr(> z )	-14.4481 < 2·10 <sup>-16</sup>	1.07935 < 2·10 <sup>-16</sup>	0.89706 < 2·10 <sup>-16</sup>	0.14725 6.96·10 <sup>-6</sup>	5.14	772.48	4.76	3.50
Single-Exposure	-	Estimate Pr(> z )	-10.9108 < 2·10 <sup>-16</sup>	0.85442 2.26·10 <sup>-11</sup>	0.76618 < 2·10 <sup>-16</sup>	- -	4.12	788.96	4.85	3.48
(c) Free road segments										
Model	Consistency parameter		$\beta_0$ -	$\beta_1$ $\ln L$	$\beta_2$ $\ln AADT$	$\beta_3$ $C$	Overdispersion $\theta$	AIC	RMSE	MAE
L <sub>400,0</sub>	7	Estimate Pr(> z )	-11.5246 8.96·10 <sup>-8</sup>	0.83835 2.43·10 <sup>-5</sup>	0.72643 7.62·10 <sup>-7</sup>	0.18064 6.67·10 <sup>-4</sup>	116	204.86	2.16	1.76
t <sub>15,6</sub>	7	Estimate Pr(> z )	-11.6067 4.75·10 <sup>-8</sup>	0.83255 2.12·10 <sup>-5</sup>	0.74202 3.86·10 <sup>-7</sup>	0.22636 3.93·10 <sup>-4</sup>	168	203.79	2.14	1.72
L <sub>400,0</sub>	8	Estimate Pr(> z )	-12.5705 8.86·10 <sup>-8</sup>	0.91496 1.15·10 <sup>-5</sup>	0.79753 4.44·10 <sup>-7</sup>	0.14399 8.45·10 <sup>-4</sup>	69	204.93	2.19	1.82
t <sub>15,6</sub>	8	Estimate Pr(> z )	-12.6155 4.79·10 <sup>-8</sup>	0.90608 1.02·10 <sup>-5</sup>	0.80286 2.29·10 <sup>-7</sup>	0.17887 5.10·10 <sup>-4</sup>	80	204.02	2.18	1.77
Single-Exposure	-	Estimate Pr(> z )	-8.3791 2.98·10 <sup>-4</sup>	0.7015 2.33·10 <sup>-3</sup>	0.5710 7.22·10 <sup>-4</sup>	- -	11.18	212.49	2.24	1.80
Variable is significant when Pr(> z ) < 0.05										
*Model is defined by X <sub>i,j</sub> , where X is L when the model is based on distance and t when the model is based on time; i represents the distance (m) or time (s) used for the calculation of the inertial operating speed; and j is the value of α considered in the weighting distribution.										

318 **5. GLOBAL CONSISTENCY MODEL**

319 A new global consistency model was proposed based on the previous results. In this way, the consistency  
 320 parameter 7 was preferred as the global consistency parameter compared to parameter 8. This was because  
 321 all variables used by parameter 7 were based on the positive differences between V<sub>i</sub> and V<sub>85</sub>, which represent  
 322 where drivers' expectancies were not fulfilled. Therefore, this parameter is more consistent than parameter  
 323 8 and better represents the studied phenomenon.

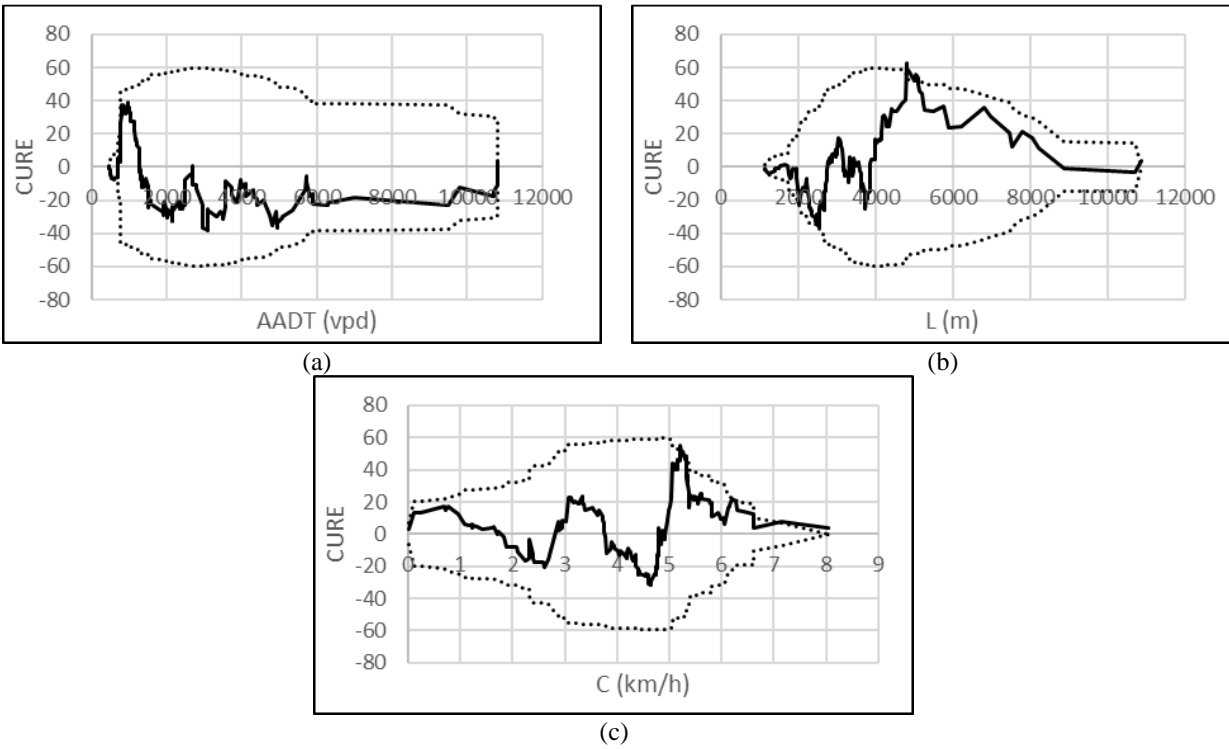
324 Likewise, a time-based inertial operating speed profile was proposed. Thus, the inertial operating  
325 speed should be calculated at each point of the alignment as the weighted average operating speed of the  
326 preceding 15 s considering a linear weighting distribution. This distribution was selected because of its  
327 simplicity.

328 Thus, Equation 4 shows the Safety Performance Function which allows estimating the number of  
329 crashes on an entire homogeneous road segment. It should be highlighted that this SPF also showed  
330 favorable values of goodness of fit ( $AIC=978$ ;  $RMSE=4.39$ ;  $MAE=3.11$ ).

$$331 Y_{i,10} = e^{-6.6479} \cdot L^{1.02645} \cdot AADT^{0.86684} \cdot e^{0.14774 \cdot C} \quad (4)$$

332 The quality of fit was also studied from the Cumulative Residuals (CURE) Plots (Hauer and Bamfo,  
333 1997; Lord and Persaud, 2000). This method consists of plotting the cumulative residuals for each  
334 independent variable. The aim is to graphically observe how well the function fits the data set. The CURE  
335 method has the advantage of not being dependent on the number of observations, as many other traditional  
336 statistical procedures are. In general, a good CURE plot is one that oscillates around 0. Thus, a good fit is  
337 given when the residuals do not stray beyond the  $\pm 2\sigma^*$  boundaries.

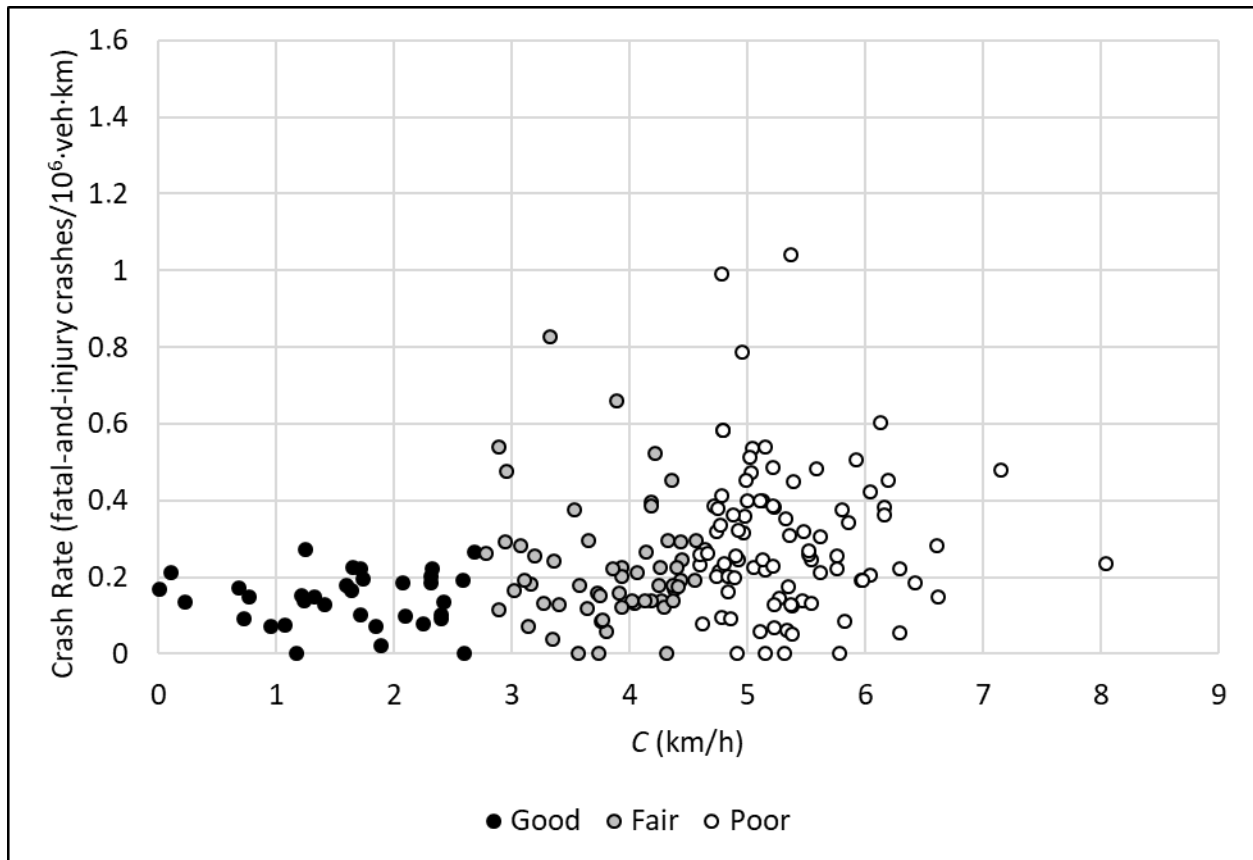
338 It can be observed that the plots against each explanatory variable did not stray beyond the  $\pm 2\sigma^*$   
339 boundaries (Figure 5). Therefore, the proposed SPF is a useful tool to estimate the number of crashes on  
340 Spanish two-lane rural roads.



341  
342 **FIGURE 5 CURE plots: (a) AADT; (b) Length; (c) Consistency.**

343 Figure 6 shows the relationship between the global consistency parameter ( $C$ ) and crash rates,  
344 which were calculated considering observed crashes. To this regard, crash rate increases with the  
345 consistency parameter. These results are consistent with the studied phenomenon, since the higher the  
346 difference between drivers' expectancies and road behavior, the higher the likelihood of crash occurrence.

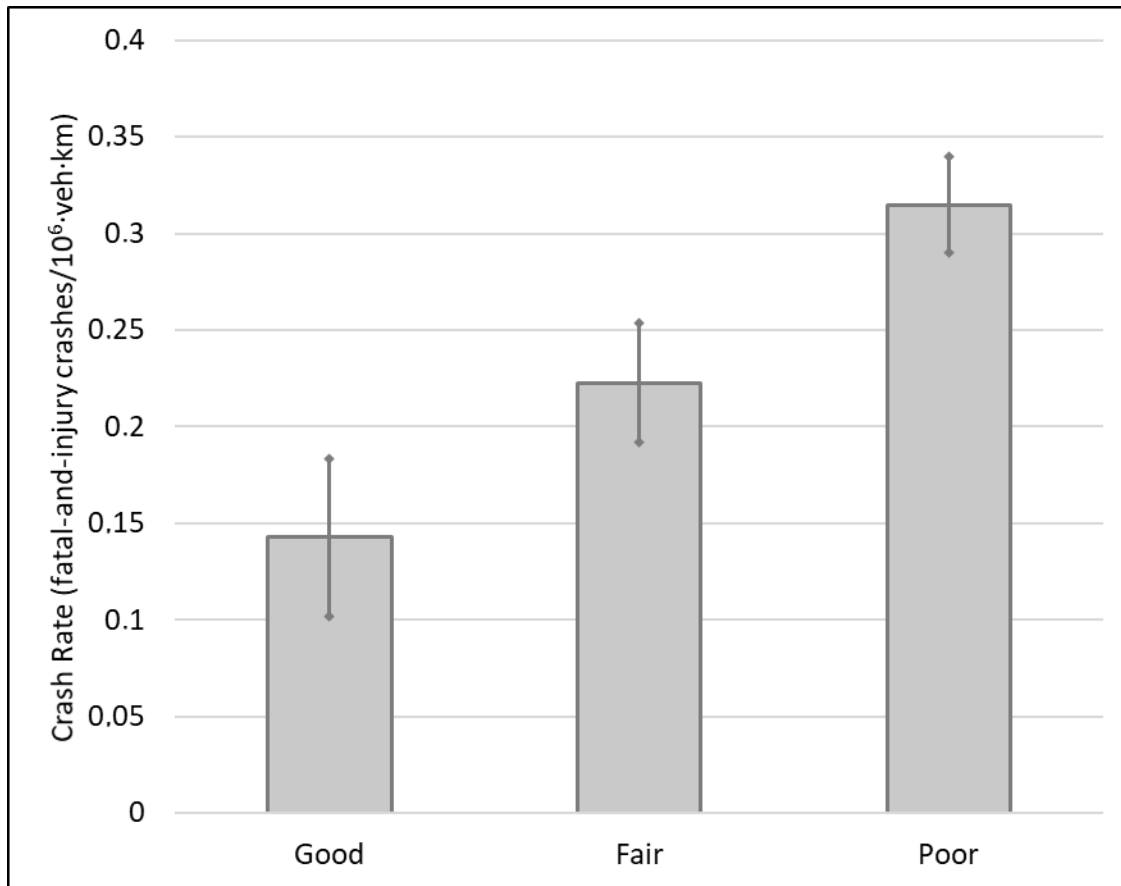
347 Three consistency levels were defined by means of a cluster analysis. Regarding this, the studied  
348 road segments were classified into three groups considering the values of the consistency parameters  
349 through a k-means clustering, which used the squared Euclidean distance as a measure of cluster scatter.  
350 As a result, a homogenous road segment has a good consistency level when the consistency parameter  $C$  is  
351 lower than 2.75 km/h, a poor consistency level when  $C$  is higher than 4.5 km/h, and a fair consistency level  
352 in all other cases (Figure 6 and Figure 7).



353

354 **FIGURE 6 Global consistency model Vs. Crash rates.**

355 In addition, the average crash rate was analyzed considering the defined consistency thresholds  
356 (Figure 7). A statistical test showed significant differences between these consistency levels at a 90%  
357 confidence level, so the proposed global consistency model can properly assess road safety on an entire  
358 road segment, and distinguish between the proposed consistency thresholds.



359  
360 **FIGURE 7 Average crash rate Vs. Consistency level.**

## 361 **6. DISCUSSION**

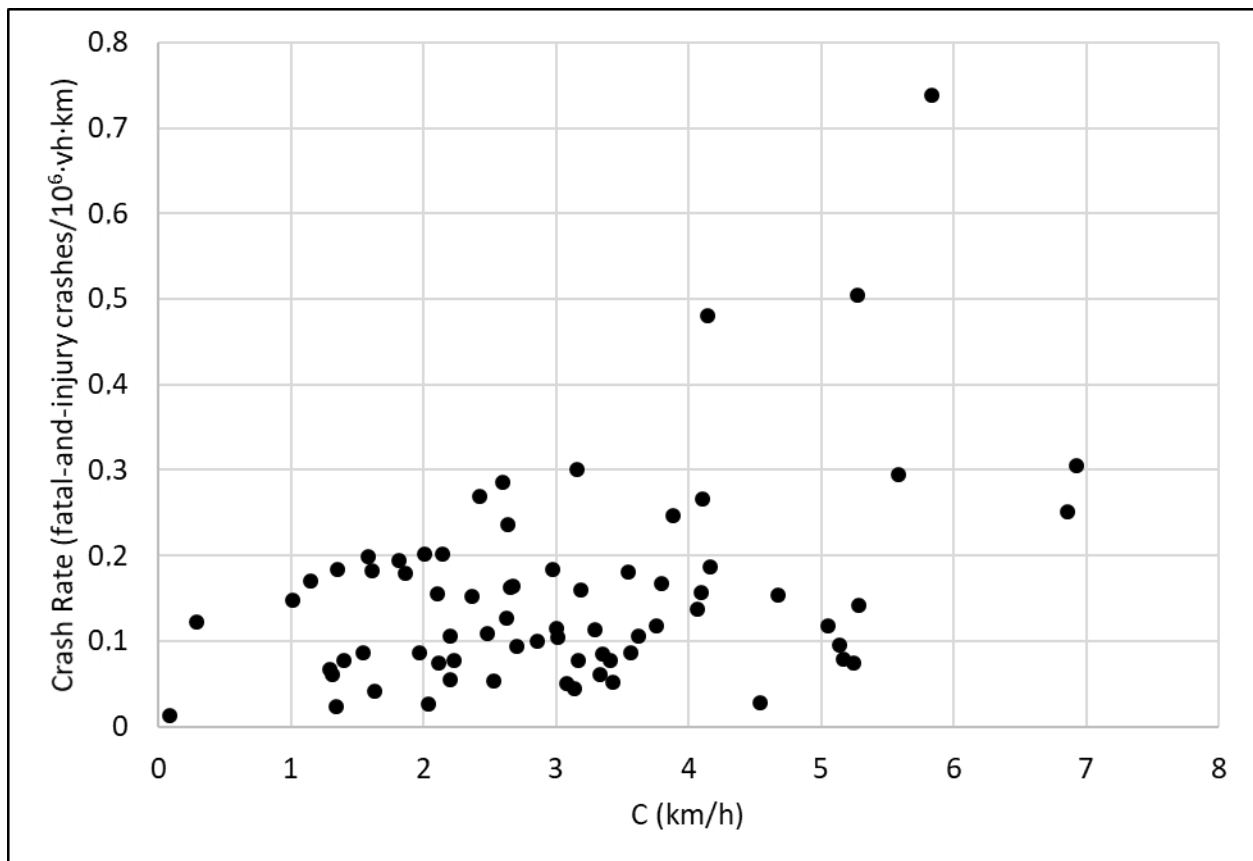
### 362 **6.1. Drivers' expectancies acquirement process**

363 A time-based inertial operating speed profile showed more robust results than those based on distance. This  
364 is consistent with the results obtained on Italian highways (Llopis-Castelló et al. 2018) and validates the  
365 hypothesis that drivers' expectancies acquirement process is closely related to Short-Term Memory (STM).  
366 In addition, the best results were achieved considering 15 s, which was very close to 18 s referred by Revlin,  
367 (2012) for Short-Term Memory.

368 On the other hand, this period of time is lower than 25 s which was obtained on Italian two-lane  
369 rural roads (Llopis-Castelló et al., 2018). This might be associated with driver workload. To this regard, the  
370 average Curvature Change Rate (*CCR*) of the homogeneous road segments used in this research (209  
371 gon/km) was higher than those observed on Italian highways (91 gon/km), hence requiring a higher driver  
372 workload.

373 However, the proposed SPF in this study was applied to Italian two-lane rural roads considered by  
 374 Llopis-Castelló et al. (2018a and 2018b). Thus, it should be highlighted that the indexes of goodness of fit  
 375 obtained ( $RMSE=22.5$ ;  $MAE=15.45$ ) were similar to those obtained applying the SPF developed with Italian  
 376 data ( $RMSE=21.64$ ;  $MAE=13.75$ ).

377 In addition, the relationship between the proposed consistency parameter and crash rates was  
 378 analyzed (Figure 8). The results obtained were consistent with those observed in this research, i.e., the  
 379 higher the consistency parameter, the higher the crash rate. As a conclusion, the new model revealed a  
 380 favorable performance on Italian two-lane rural roads.



381  
 382 **FIGURE 8 Global consistency model Vs. Crash rates on Italian highways.**

### 383 6.2. Consistency parameter

384 The consistency parameter  $C$  is based on the combination of the following, simpler parameters:  $\sqrt{\frac{A(+)\sigma(+)}{L(+)}}$ .

385  $A(+)$  is the bounded area within the  $V_i$  and  $V_{85}$  profiles considering only the positive differences,  $L(+)$  is  
 386 the length of the road segment for which  $V_i$  is higher than  $V_{85}$ , and  $\sigma(+)$  is the standard deviation of the

387 difference between  $V_i$  and  $V_{85}$  profile considering only the positive differences.

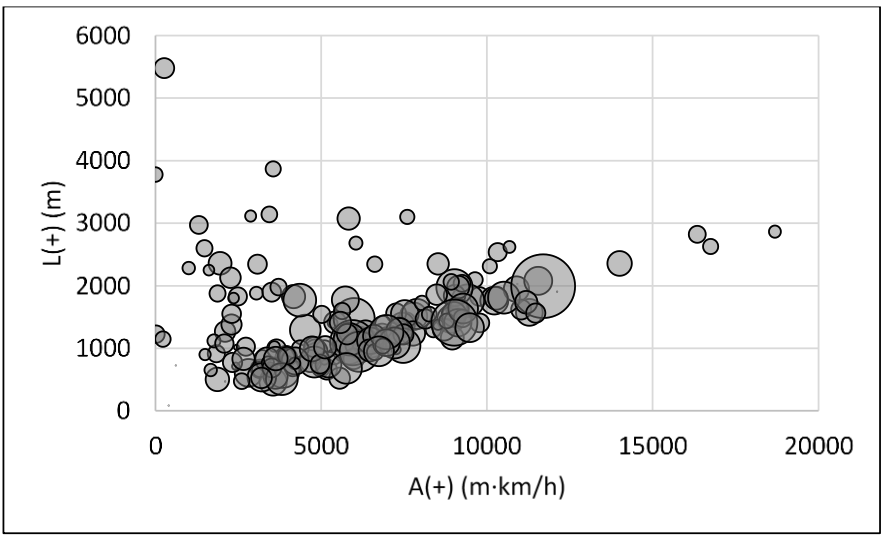
388 Figure 9 shows the relationship between these parameters, where each point is a homogeneous road  
389 segment (size is related to crash rate). In this way, the biggest points were concentrated for great values of  
390  $A(+)$  and low values of  $L(+)$  (Figure 9a). This is consistent with the definition of the consistency parameter,  
391 since a large  $C$  is associated with a lower consistency level and, consequently, the likelihood of crash  
392 occurrence is greater.

393 Likewise, the greater the  $A(+)$  or  $\sigma(+)$ , the larger the crash rate (Figure 9b). To this regard, both  
394 variables are directly proportional to  $C$ , so an increase of any of them leads to a greater likelihood of crash  
395 occurrence, i.e., a lower consistency level.

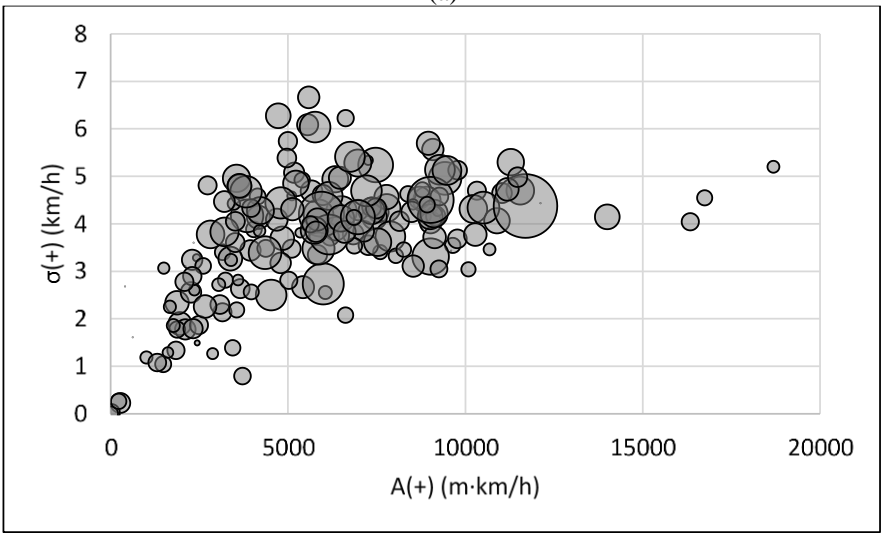
396 Finally, the relationship between  $L(+)$  and  $\sigma(+)$  was also studied (Figure 9c). This is not as intuitive  
397 as the previous ones due to  $A(+)$  is the main variable, i.e.,  $L(+)$  and  $\sigma(+)$  help to better understand the  
398 studied phenomenon. For example, given two homogeneous road segments with similar  $A(+)$ , the segment  
399 showing either lower  $\sigma(+)$  or larger  $L(+)$  will be more consistent. Related to this, road segments with greater  
400 crash rates are concentrated for higher  $\sigma(+)$  and lower  $L(+)$ .

401 As a conclusion, the variables which define the new global consistency parameter can properly  
402 quantify how drivers' expectancies and road behavior relate. Therefore, the proposed parameter  $C$  is a good  
403 surrogate measure of geometric design consistency.

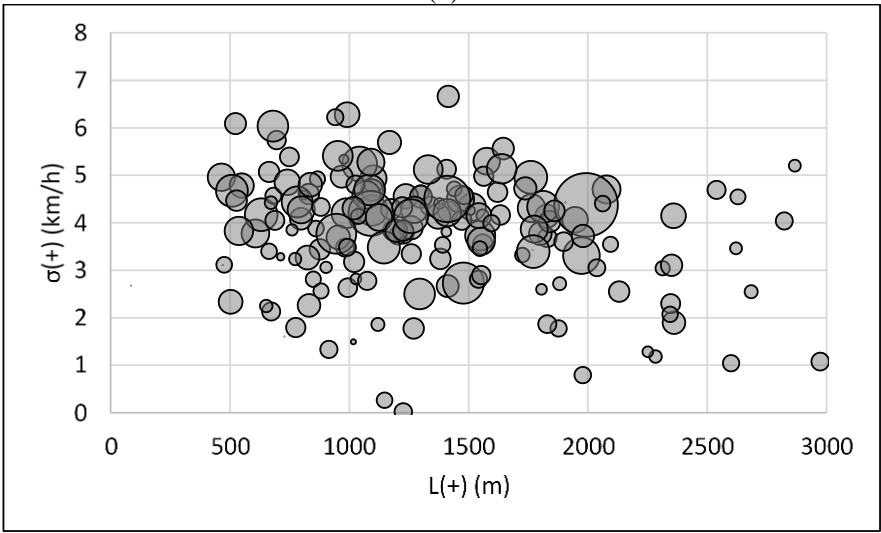




(a)



(b)



(c)

404  
405

**FIGURE 9** Consistency parameter analysis.

406

407 **6.3. Validation of the proposed global consistency model**

408 The new global consistency model was validated considering 26 homogeneous road segments different  
 409 from the road segments used for the calibration of the model. These were randomly selected among a total  
 410 of 105 homogeneous road segments. Table 6 shows a summary of the main characteristics of these road  
 411 segments.

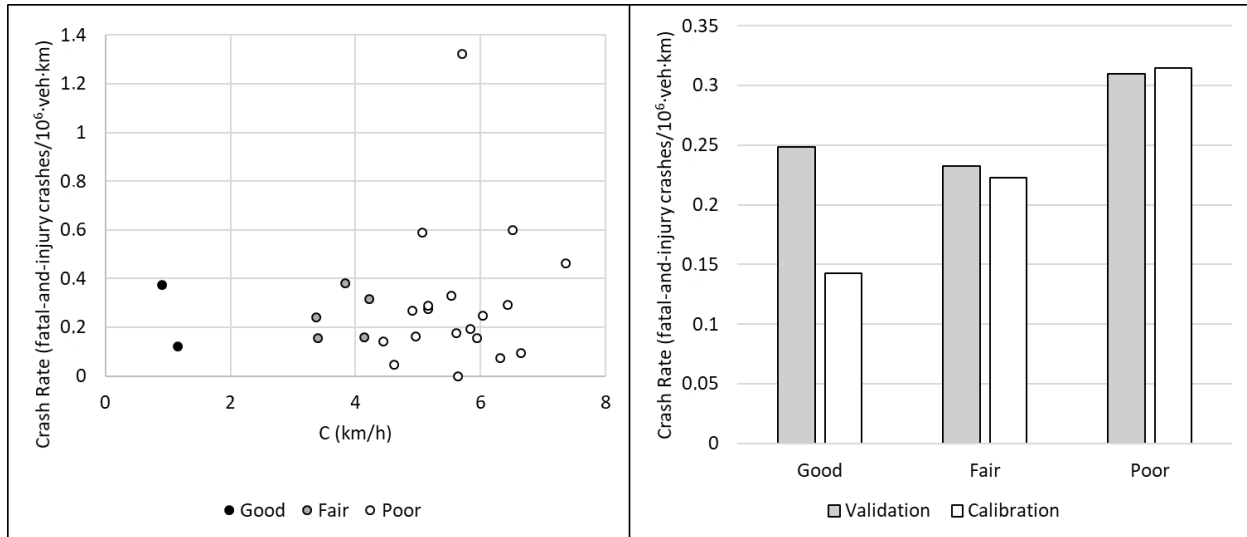
412 **TABLE 6 Statistical summary of the homogeneous road segments used for the validation**

	Minimum	Maximum	Average	Standard deviation
Length (m)	1,054	5,472	2,803	1,237
CCR (gon/km)	8.69	697.07	164.76	160.06
AADT (vpd)	518	7,022	2,411	1,754
Crashes	0	31	6.69	7.66

413

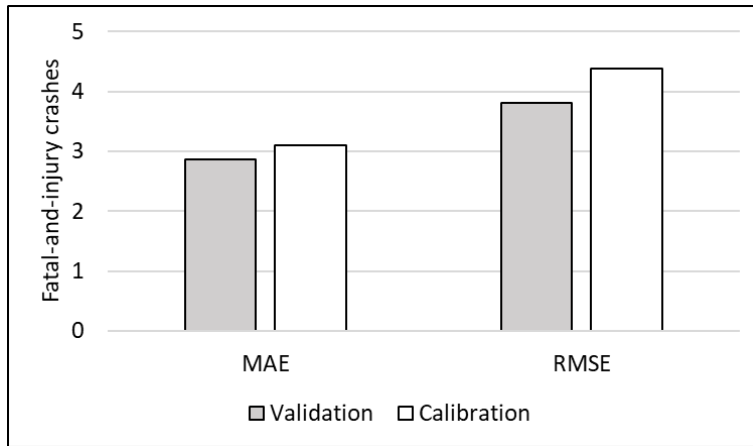
414 The geometry of these road segments was recreated by means of the methodology proposed by  
 415 Camacho-Torregrosa et al. (2015), whereas the operating speed profile of each of them was estimated  
 416 considering the operating speed models developed by Pérez-Zuriaga (2012). According to the results  
 417 obtained previously, the inertial operating speed profiles were calculated through the weighted average  
 418 operating speed of the preceding 15 seconds considering a linear weighting distribution.

419 Finally, the consistency parameter  $C$  was obtained for each homogeneous road segment. The  
 420 correlation between this parameter and crash rate was analyzed (Figure 10). The average crash rates for fair  
 421 and poor consistency levels obtained in the validation process were similar to those obtained in the  
 422 calibration of the model, whereas the average crash rate for a good consistency level in the validation was  
 423 larger than that obtained in the calibration. This is due to the few homogeneous road segments with good  
 424 consistency level.



425  
426 **FIGURE 10 Validation of the consistency model: Crash Rate Vs. Consistency.**

427 Additionally, the relationship between the observed and predicted crashes was analyzed by  
428 comparing the parameters of goodness of fit (*MAE* and *RMSE*) obtained in the validation and calibration  
429 process (Figure 11). To this regard, the predicted fatal-and-injury crashes were estimated considering the  
430 SPF defined for the new consistency model (Equation 4). Both *MAE* and *RMSE* were lower in the validation  
431 process, which verifies the sturdiness of the new consistency model.



432  
433 **FIGURE 11 Validation of the consistency model: Observed crashes Vs. Predicted crashes.**

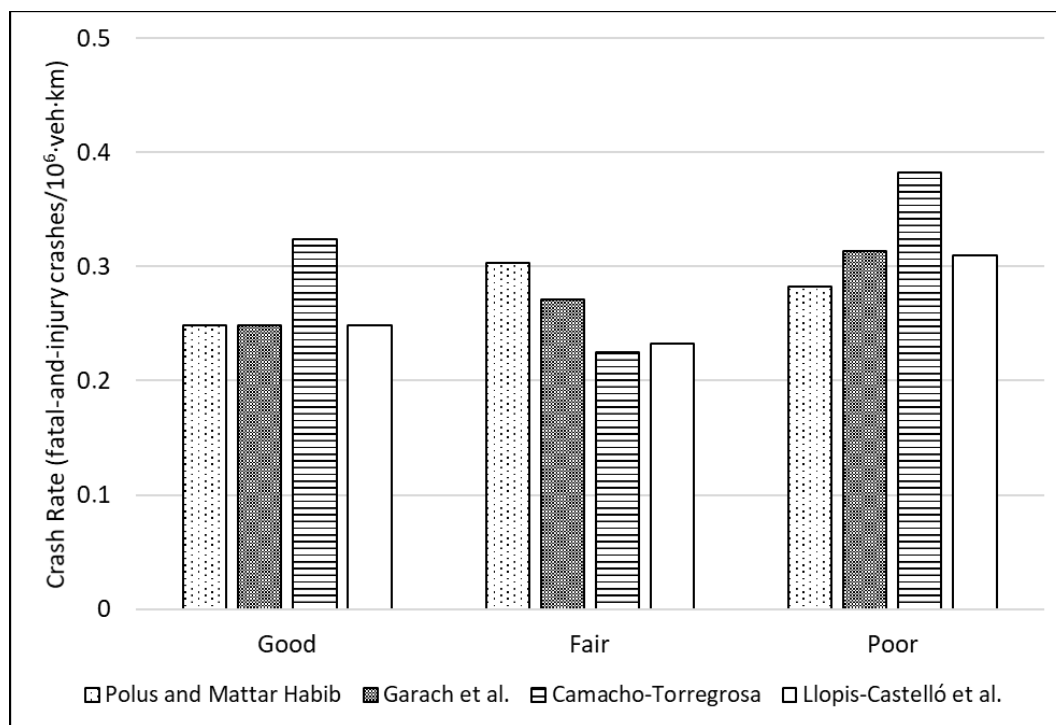
434 As a conclusion, the proposed global consistency model assesses properly the consistency level and can be  
435 used to estimate the number of fatal-and-injury crashes on an entire homogeneous road segment.

436 **6.4. Comparison with previous consistency models**

437 The new global consistency model was compared with the models developed by Polus and Mattar-Habib  
438 (2004), Garach et al. (2014), and Camacho-Torregrosa (2015). All consistency parameters were obtained

439 for each homogeneous road segment and the average crash rate was calculated for each consistency level  
 440 (Figure 12). To do this, only the homogeneous road segments used for the validation of the model were  
 441 considered.

442 As mentioned above, only two homogeneous road segments showed good consistency, so this  
 443 consistency level was not considered in the analysis. Thus, the consistency models which can better  
 444 represent the studied phenomenon are the models developed by Camacho-Torregrosa (2015) and the model  
 445 proposed in this research, since significant statistical differences were identified between the average crash  
 446 rate for a fair and poor consistency level at a 95% confidence level. However, the models proposed by Polus  
 447 and Mattar-Habib (2004) and Garach et al. (2014) resulted in very similar average crash rates for these  
 448 consistency levels. In addition, the average crash rate observed for a fair consistency was greater than that  
 449 for a poor consistency considering the model developed by Polus and Mattar-Habib (2004), which is not  
 450 consistent with the studied phenomenon.

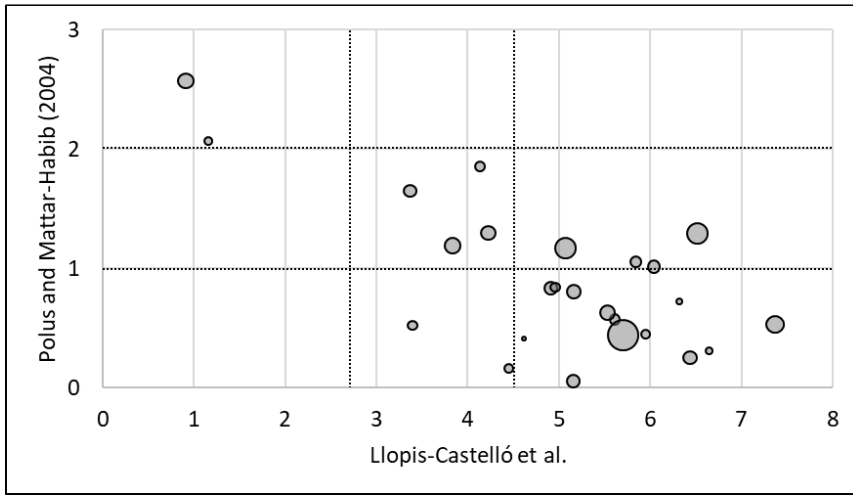


451  
 452 **FIGURE 12 Average crash rate Vs. Consistency level of previous models.**

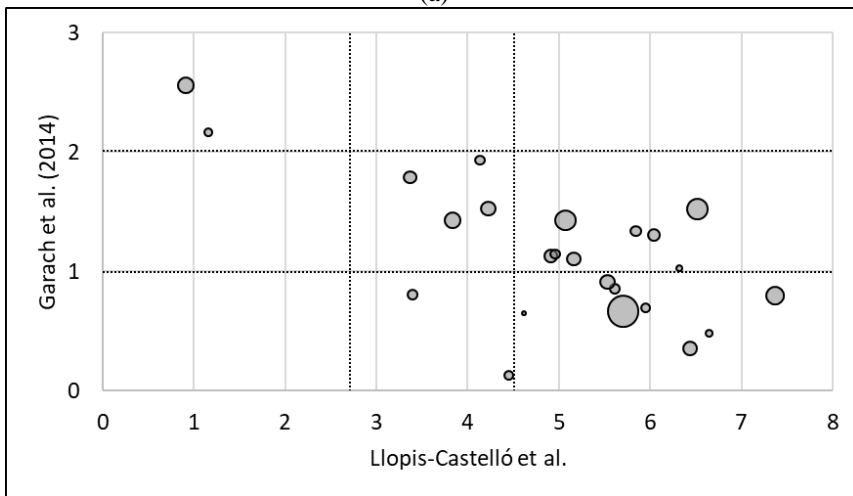
453 To better understand these results, the relationship between the proposed consistency parameter  
 454 and the consistency parameters developed by the other authors was analyzed. In Figure 13, each point is a

455 homogeneous road segment and its size represents its crash rate. The larger the size, the greater the crash  
456 rate. Likewise, the dotted lines represent the consistency thresholds of the different consistency models.

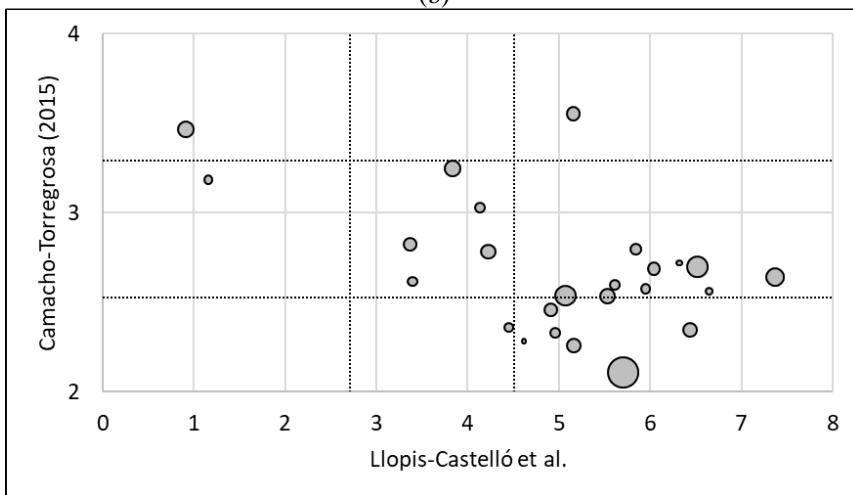
457 Thus, it was identified that the consistency models developed by Polus and Mattar-Habib (2004)  
458 and Garach et al. (2014) presented points with very different size within the same consistency level.  
459 Particularly, some homogeneous road segments with high crash rates were labeled with a fair consistency  
460 level. This explained that the average crash rates for this consistency level were larger than those obtained  
461 with the proposed consistency model in this research and the model developed by Camacho-Torregrosa  
462 (2015). In addition, the model proposed by Polus and Mattar-Habib et al. (2004) defined some  
463 homogeneous road segments with low crash rates with a poor consistency level, which explained why the  
464 average crash rate associated with this consistency level was much lower than those obtained from the other  
465 models.



(a)



(b)



(c)

466  
 467 **FIGURE 13 Proposed consistency parameter Vs. Previous consistency parameters: (a) Polus and**  
 468 **Mattar-Habib (2004); (b) Garach et al. (2014); (c) Camacho-Torregrosa (2015).**

## 469 6.5. SPF based on consistency Vs. SPF based on alignment indexes

470 Finally, the new SPF based on consistency was compared with a SPF based on the geometric parameter  
 471 Curvature Change Rate (*CCR*), which represents how winding a homogenous road segment is. To this  
 472 regard, a great *CCR* is related to homogeneous road segments with shorter tangents and sharper curves,  
 473 which usually leads to greater speed variations.

474 Table 7 shows the statistical adjustment for the SPF based on *CCR* and consistency. As a result, the  
 475 SPF based on consistency is able to more accurately estimate the number of crashes, since the parameters  
 476 of goodness of fit for the SPF based on *CCR* are significantly greater than those obtained for the new global  
 477 consistency model. Additionally, *CCR* resulted in a non-significant variable because the parameter  $\Pr(>|z|)$   
 478 was higher than 0.05.

479 **TABLE 7 Statistical adjustment – Global consistency models**

		$\beta_0$	$\beta_1$	$\beta_2$	$\beta_3$	Overdispersion $\theta$	<i>AIC</i>	<i>RMSE</i>	<i>MAE</i>
		-	$\ln L$	$\ln AADT$	<i>CCR</i>				
SPF based on <i>CCR</i>	Estimate $\Pr(> z )$	-5.1064 < $2 \cdot 10^{-16}$	0.85071 $7.15 \cdot 10^{-14}$	0.77578 < $2 \cdot 10^{-16}$	$3.069 \cdot 10^{-6}$ 0.99	4.52	993.85	4.7789	3.4499
Llopis- Castelló et al.	Estimate $\Pr(> z )$	-6.6479 < $2 \cdot 10^{-16}$	1.02645 < $2 \cdot 10^{-16}$	0.86684 < $2 \cdot 10^{-16}$	0.14774 $5.47 \cdot 10^{-7}$	5.83	978.00	4.3937	3.1078
Variable is significant when $\Pr(> z ) < 0.05$ .									

## 480 7. CONCLUSIONS AND FURTHER RESEARCH

481 This paper presents a new global consistency model based on the difference between the inertial operating  
 482 speed profile and the operating speed profile for road safety assessment on Spanish two-lane rural roads.

483 The main objective of this study was to identify how the inertial operating speed should be  
 484 calculated, which is a surrogate measure of drivers' expectancies. To this regard, distances between 300 m  
 485 and 800 m with a step of 100 m, periods of time between 10 s and 40 s with a step of 5 s, and 11 weighting  
 486 distributions were analyzed. Thus, 143 inertial operating speed profiles were calculated for each  
 487 homogeneous road segment. Likewise, 8 consistency parameters were studied, so a total of 1,144 Safety  
 488 Performance Functions were calibrated.

489 The new consistency model was defined as  $\sqrt{\frac{A(+)\sigma(+)}{L(+)}}$  (parameter 7), being  $A(+)$  the bounded area  
 490 within the  $V_i$  and  $V_{85}$  profiles,  $\sigma(+)$  the standard deviation of the difference between  $V_i$  and  $V_{85}$  profile, and  
 491  $L(+)$  the length of the road segment for which  $V_i$  is higher than  $V_{85}$ . Related to this, the inertial operating

492 speed profile was defined as the weighted average operating speed of the preceding 15 seconds considering  
493 a linear weighting distribution, which is consistent with drivers' expectancies acquirement process.

494 Additionally, it was identified that the SPFs calibrated by means of a time-based inertial operating  
495 speed profile showed more consistent results than those obtained through distance-based speed profiles.  
496 This allowed validating the results obtained for Italian two-lane rural roads (Llopis-Castelló et al., 2018b).

497 A Safety Performance Function was proposed to estimate the number of crashes on an entire  
498 homogeneous road segment and consistency thresholds were defined. In this way, a homogenous road  
499 segment have a good consistency level when the consistency parameter ( $C$ ) is lower than 2.75 km/h, a poor  
500 consistency level when  $C$  is higher than 4.5 km/h, and a fair consistency level otherwise.

501 Finally, the proposed model was compared with those developed previously by other authors. As a  
502 conclusion, the models developed by Polus and Mattar-Habib (2004) and Garach et al. (2014) were not able  
503 to properly estimate the consistency level of the road segments included in this study. Conversely, the  
504 proposed model presented a high correlation with the model developed by Camacho-Torregrosa (2015).  
505 However, the new model showed better fitting. Therefore, the proposed global consistency model better  
506 describes the phenomenon than the previous models.

507 New tools were developed which can be used by highway engineers to incorporate road safety to  
508 the geometric design of both new Spanish two-lane rural roads and improvements of existing highways.

509 Despite the important improvement over previous consistency approaches, there are some  
510 limitations remaining. The relative short length of homogeneous road segments, combined with the removal  
511 of PDO crashes, made it necessary to consider such a long period of time (10 years). Otherwise, crashes  
512 would not be Negative Binomial distributed. Shorter periods of time would be preferred, but other more  
513 complex and/or less accurate distributions should be applied instead. In addition, this consistency model  
514 applies to a limited range of cross-section and longitudinal characteristics of two-lane rural roads. Different  
515 models could be calibrated for other road types, including, e.g., low volume roads. Although the same  
516 methodology could be applied, changes in probability distribution and functional forms might be expected,  
517 because of the different crash distributions.



**518 ACKNOWLEDGMENTS**

519 The study presented in this paper is part of the research project titled “CASEFU - Estudio experimental de  
520 la funcionalidad y seguridad de las carreteras convencionales” (TRA2013-42578-P), subsidized by the  
521 Spanish Ministry of Economy, Industry and Competitiveness and the European Social Fund. In addition,  
522 the authors would like to thank the Department of Housing, Public Works and Spatial Planning of the  
523 Valencian Regional Government and the Traffic Department of the Spanish Government, which provided  
524 traffic and crash data, respectively.

**525 REFERENCES**

- 526 1. Anderson, I., K. Bauer, and D. Harwood. Relationship to safety of geometric design consistency  
527 measures for rural two-lane highways. *Transportation Research Record: Journal of the*  
528 *Transportation Research Board*, 1999, no 1658, p. 43-51.
- 529 2. Awatta, M., Y. Hassan, and T. Sayed. Quantitative evaluation of highway safety performance based  
530 on design consistency. *Advances in Transportation Studies*, 2006, vol. 9.
- 531 3. Cafiso, S., A. Di Graziano, G. Di Silvestro, G. La Cava, and B. Persaud. Development of  
532 comprehensive accident models for two-lane rural highways using exposure, geometry, consistency  
533 and context variables. *Accident Analysis & Prevention*, 2010, vol. 42, no 4, p. 1072-1079.
- 534 4. Camacho Torregrosa, F. J. Development and calibration of a global geometric design consistency  
535 model for two-lane rural highways, based on the use of continuous operating speed profiles.  
536 *Universitat Politècnica de València, Valencia (Spain)*, 2015.
- 537 5. Camacho-Torregrosa, F. J., A. M. Pérez-Zuriaga, J. M. Campoy-Ungría, A. García, and A. P.  
538 Tarko. Use of Heading Direction for Recreating the Horizontal Alignment of an Existing Road.  
539 *Computer-Aided Civil and Infrastructure Engineering*, 2015, vol. 30, no 4, p. 282-299.
- 540 6. de Oña, J., Garach, L., Calvo, F., García-Muñoz, T. Relationship between Predicted Speed  
541 Reduction on Horizontal Curves and Safety on Two-Lane Rural Roads in Spain. *Journal of*  
542 *transportation engineering*, 2013, 140(3), 04013015.
- 543 7. Dirección General de Tráfico (DGT), 2017. [http://www.dgt.es/es/seguridad-vial/estadisticas-e-](http://www.dgt.es/es/seguridad-vial/estadisticas-e-indicadores/)  
544 [indicadores/](http://www.dgt.es/es/seguridad-vial/estadisticas-e-indicadores/)
- 545 8. Garach, L., F. Calvo, M. Pasadas, and J. de Oña. Proposal of a New Global Model of Consistency:  
546 Application in Two-Lane Rural Highways in Spain. *Journal of Transportation Engineering*, 2014,  
547 vol. 140, no 8, p. 04014030.
- 548 9. Garach, L., J. de Oña, G. López, and L. Baena. Development of safety performance functions for  
549 Spanish two-lane rural highways on flat terrain. *Accident Analysis & Prevention*, 2016, vol. 95, p.  
550 250-265.
- 551 10. García, A., D. Llopis-Castelló, F. J. Camacho-Torregrosa, and A. M. Pérez-Zuriaga. New  
552 consistency index based on inertial operating speed. *Transportation Research Record: Journal of*  
553 *the Transportation Research Board*, 2013b, no 2391, p. 105-112.
- 554 11. García, A., Llopis-Castello, D., Perez-Zuriaga, A.M., Camacho-Torregrosa, F.J. Homogeneous  
555 Road Segment Identification Based On Inertial Operating Speed. In *Transportation Research Board*  
556 *92nd Annual Meeting*, 2013a, No. 13-3545.
- 557 12. Gibreel, G. M., S. M. Easa, Y. Hassan, and I. A. El-Dimeery. State of the art of highway geometric  
558 design consistency. *Journal of Transportation Engineering*, 1999, vol. 125, no 4, p. 305-313.
- 559 13. Hauer, E., and J. Bamfo. Two tools for finding what function links the dependent variable to the  
560 explanatory variables. *Proceedings of the ICTCT 1997 Conference, Lund, Sweden. 1997.*

- 561 14. Llopis-Castelló, D., F. Bella, F. J. Camacho-Torregrosa, and A. García. New consistency model  
562 based on inertial operating speed profiles for road safety evaluation. *Journal of Transportation*  
563 *Engineering*, 2018a, 144(4), 04018006.
- 564 15. Llopis-Castelló, D., F. Bella, F. J. Camacho-Torregrosa, and A. García. Time-based calibration of  
565 the inertial operating speed to enhance the assessment of the geometric design consistency.  
566 *Transportation Research Record: Journal of the Transportation Research Board*, 2018b, Accepted.
- 567 16. Lord, D., and B. N. Persaud. Accident prediction models with and without trend: application of the  
568 generalized estimating equations procedure. *Transportation Research Record: Journal of the*  
569 *Transportation Research Board*, 2000, no 1717, p. 102-108.
- 570 17. Lord, D., and F. Mannering. The statistical analysis of crash-frequency data: a review and  
571 assessment of methodological alternatives. *Transportation Research Part A: Policy and Practice*,  
572 2010, vol. 44, no 5, p. 291-305.
- 573 18. Mehta, G., and Lou, Y. (2013). "Calibration and Development of Safety Performance Functions  
574 for Alabama." *Transportation Research Record: Journal of the Transportation Research Board*,  
575 Volume 2398, 75–82.
- 576 19. Misaghi, P., Hassan, Y. Modeling Operating Speed and Speed Differential on Two-Lane Rural  
577 Roads. *Journal of Transportation Engineering*, 2005, 131(6), 408-418.
- 578 20. Montella, A., and L. L. Imbriani. Safety performance functions incorporating design consistency  
579 variables. *Accident Analysis & Prevention*, 2015, vol. 74, p. 133-144.
- 580 21. Montella, A., L. Colantuoni, and R. Lamberti. Crash prediction models for rural motorways.  
581 *Transportation Research Record: Journal of the Transportation Research Board*, 2008, no 2083, p.  
582 180-189.
- 583 22. Ng, J., and T. Sayed. Effect of geometric design consistency on road safety. *Canadian Journal of*  
584 *Civil Engineering*, 2004, vol. 31, no 2, p. 218-227.
- 585 23. Pérez-Zuriaga, A.M. Caracterización y modelización de la velocidad de operación en carreteras  
586 convencionales a partir de la observación naturalística de la evolución de vehículos ligeros.  
587 *Universitat Politècnica de València, Valencia (Spain)*, 2012.
- 588 24. Polus, A., and C. Mattar-Habib. New consistency model for rural highways and its relationship to  
589 safety. *Journal of transportation engineering*, 2004, vol. 130, no 3, p. 286-293.
- 590 25. Quddus, M. Exploring the relationship between average speed, speed variation, and accident rates  
591 using spatial statistical models and GIS. *Journal of Transportation Safety & Security*, 2013, vol. 5,  
592 no 1, p. 27-45.
- 593 26. Resende, P., and R. Benekohal. Effect of roadway section length on accident modeling traffic  
594 congestion and traffic safety. *The 21 st Century Conference, ASCE, Chicago, IL*. 1997.
- 595 27. Revlin, R. *Cognition: Theory and practice*. Palgrave Macmillan, 2012.
- 596 28. Srinivasan, R., Colety, M., Bahar, G., Crowther, B., and Farnen, M. (2016). "Estimation of  
597 Calibration Functions for Predicting Crashes on Rural Two-Lane Roads in Arizona."  
598 *Transportation Research Record: Journal of the Transportation Research Board*, Volume 2583,  
599 17–24.
- 600 29. Treat, J. R., N. S. Tumbas, S. T. McDonald, D. Shinar, and R. D. Hume. Tri-level study of the  
601 causes of traffic accidents: Executive summary (National Technical Information Services Technical  
602 Report No. DOT HS-805 099). Bloomington: University of Indiana, 1979.
- 603 30. WHO. *Global status report on road safety 2015*. World Health Organization, 2015.
- 604 31. Wu, K.-F., E. T. Donnell, S. C. Himes, and L. Sasidharan. Exploring the association between traffic  
605 safety and geometric design consistency based on vehicle speed metrics. *Journal of Transportation*  
606 *Engineering*, 2013, vol. 139, no 7, p. 738-748.